An Optimization and Characterization Study on Sodium Ferrate Production by Electrochemical Method

Sina Samimi-Sedeh, Ehsan Saebnoori *, Ali Hassanzadeh

Advanced Materials Research Center, Department of Materials Engineering, Najafabad Branch, Islamic Azad University, Najafabad, Iran.

ARTICLE INFO

Article history:

Received 20 March 2020
Accepted 12 April 2020
Available online 15 April 2020

Keywords:

Electrochemical method
Sodium ferrate
Alkaline solution
Current efficiency
Energy consumption

ABSTRACT

Current efficiency and energy consumption are two important factors in sodium ferrate synthesis. In this article, sodium ferrate was produced by the electrochemical method and the effects of different synthesized parameters such as applied current density, sodium hydroxide concentration and temperature on current efficiency and energy consumption have been studied. Decomposition of sodium ferrate, anode passivation and deviations in anodic and cathodic reaction rates with time have been tested by weight loss test, potentiodynamic polarization, and UV-visible spectroscopy, respectively. Also, the impact of each one on current efficiency and its consequence on energy consumption rate were studied. The results showed that the optimum conditions were 3.94 mA/cm^2, 16 M NaOH and 50 ^{o}C for applied current density, sodium hydroxide concentration, and temperature, respectively. In this situation, the current efficiency was calculated as 91.7% and the energy consumption reached 1.91 kW.h/kg.

1-Introduction

The effects of different parameters on ferrate (VI) synthesis through electrochemical methods have been widely studied [1]. Current efficiency and energy consumption are two important factors in sodium ferrate production which play an important role in the determination of the production rate. Anode passivation [2-6], sodium ferrate decomposition [7, 8] and increase in rate of cathodic reactions (e.g. hydrogen reduction [9] and oxygen evolution [2]) [1] in respect to anodic dissolution reaction rate lead to decline in current efficiency and increase the energy consumption in electrosynthesis of sodium ferrate. In all of these studies, the portion of each factor has not addressed to amount of deviations in current efficiency and energy consumption. It is the motivation of this article to determine the effective factors on current efficiency and energy consumption of sodium ferrate synthesis. Iron typically occurs as a metal, or in the valence states Fe (II) or Fe (III), but, more than three stable forms of iron oxidation states of 0, 2 and 3, the high oxidative environments can produce higher oxidation state of 4, 5, 6 and 8. The higher oxidation state of iron, often known as ferrate. Among them, iron with the oxidation state of 6 (FeO_4^{2-}) called ferrate (VI) which has more stability and ease of synthesis. Three following methods have mainly applied for producing ferrate (VI) (i) dry oxidation of iron at high temperature, (ii) wet oxidation of iron (III) by a chemical oxidant, and (iii) electrochemical method [10].

The electrochemical synthesis of ferrate (VI) is more common than chemical production and has a simple process that does not need any complex

* Corresponding author:
E-mail address: ehsan.saebnoori@gmail.com

or expensive reactants [9]. The electrochemical process of ferrate (VI) synthesis needs a consumable iron anode, a strong alkaline solution such as sodium or potassium hydroxide in an electrolysis cell also, electrical current for the oxidation of iron to ferrate (VI) [9]. Reactions 1 to 5 shows the synthesis steps of ferrate (VI) by electrochemical method.

$$Fe + 8OH^- \rightarrow FeO_4^{2-} + 4H_2O + 6e^- \quad (1)$$

$$Fe + 2OH^- + H_2O \rightarrow FeO_4^{2-} + 3H_2 \quad (2)$$

$$6H_2O + 6e^- \rightarrow 3H_2 + 6OH^- \quad (3)$$

$$FeO_4^{2-} + 2Na^+ \rightarrow Na_2FeO_4 \quad (4)$$

$$FeO_4^{2-} + 2K^+ \rightarrow K_2FeO_4 \quad (5)$$

Different mechanisms for ferrate (VI) synthesis have been proposed. It consists of three steps (i) formation of transient compounds, (ii) formation of ferrate (VI) particles and electrode passivation, and (iii) formation of passive layer inhibits further ferrate (VI) production [11].

Due to being a proper oxidation, sanitation, and strong coagulation properties, ferrate (VI) has been using for water treatment [12, 13], removing heavy metals [14], and corrosive ions [15], oxidation of organic substrates and degradation of organic synthetic pollutants [16, 17], corrosion inhibitor compounds in primer coating [18], steel anodizing [19], etc.

In a strong alkaline solution, the ferrate (VI) production rate depends on the amount of iron oxide and initial ferrate (VI) ion, hydroxide concentration, temperature, nickel (II) and cobalt (II) contamination, oxide film thickness and the formed hydroxide on the anode surface during the process (passivation).

In the electrochemical synthesis of ferrate (VI), the current efficiency (η) decreases by the time due to passivation and besides it diminishes by ferrate (VI) decomposition to Fe (II) and Fe (III) and in the following the ferrate (VI) decomposition enhanced by entering the Fe (II) and Fe (III) into the electrolyte [2].

Generally, ferrate (VI) spontaneously decomposes according to the reaction (6) and it shows that ferrate (VI) is unstable in the solution. The decomposition rate strongly depends on initial ferrate (VI) concentration, pH, and ions in the solution, alkalinity, and temperature [1].

$$2Feo_4^{2-} + 5H_2O \rightarrow 2Fe(OH)_3 + 4OH^- + 3/2O_2 \quad (6)$$

Electrode passivation is a common phenomenon in the electrochemical synthesis of ferrate (VI) which consists of thin film formation on anode surface and prevents the electron transfer to the electrolyte in the surface and consequently, the electrochemical reaction gradually is being stopped [20]. This film can consist of iron oxide and hydroxide layers [6] and/or a formed layer of oxygen on iron anode [8]. In alkaline solutions, the main effect of an increasing pH on film formation is a thickening of the passive film, basically because iron oxides are more stable in alkaline solutions [21]. Stainless steel which is mostly used as a cathode has similar behavior in alkaline solution. Then again, due to have some alloying elements such as chromium, nickel, etc., the formed passive film on the surface of stainless steel is more stable than carbon steel [22]. The amount of ferrate (VI) which has produced in strong alkaline electrolytes depends on the composition and structure of the passive film. The formed passive layer on the anode surface includes a double layer structure with a Fe_3O_4 interlayer and a Fe_2O_3 outer layer. The inner layer gradually dissolved in strong alkaline electrolytes step by step. In contrast, the outer layer progressively thickens which can be accompanied by more porosity and disorderliness in the passive film. The increase in porosity extension leads to less protectiveness of the passive layer and an increase in corrosion. Accordingly, the ferrate (VI) synthesis process takes placeat a higher speed [6].

2. Experimental Procedure

The anode material is selected from a sheet of carbon steel with a surface area of 24 cm^2. The cathode was stainless steel in the form of a sheet with a dimension of 80×50×0.5 mm which is curved around the anode. The composition of anode and cathode is given in table 1.

Table 1. Anode and cathode composition.

Materials	Chemical composition (wt. %)										
	Ni	Cr	S	P	Mn	Si	C	Mo	Al	Co	Fe
cathode	7.30	19.3	0.01	0.028	1.81	0.29	0.06	0.1	0.01	0.201	balance
Anode	0.005	0.025	0.014	0.022	0.187	0.045	0.047	0.013	0.022	0.002	balance

The effects of parameters of NaOH concentration, applied current density and temperature on synthesized ferrate (VI) in 30 m were studied. For test design, a parameter was maintained fix and the other was changing; in this way, first, the parameter of concentration and temperature kept fixed and the effect of applied current density on the ferrate (VI) synthesis was studied. Then, the effect of electrolyte concentration and subsequently the effect of temperature was considered.

A UV-visible spectrophotometer instrument, model OPTIZEN 3220UV, was utilized for the determination of synthesized sodium ferrate concentration in the electrolyte. For optimizing parameters of sodium ferrate production, NaOH with a purity of 98% from Nirouchlorand double distilled water from Sky Company were used. The sodium ferrate with 97% purity from Aldrich was used to prepare the calibration curve.

During the test, the temperature of the process cell is maintained with a water cooling system. In all tests, the electrolyte was agitated with a magnetic stirrer with a constant rotation speed of 350 rpm to keep the temperature and electrolyte composition uniform.

For electrochemical experiments, The PRINCETON PARSTAT 2273 with three electrode system has been utilized. The corrosion rate measurement of carbon steel has been performed in NaOH solution with different concentrations and temperatures. The working electrode was mounted in resin and let 1 cm^2 surface area be free on exposure to the solution. The electrode surface was abraded by emery-paper up to 1200 SiC grade; then, rinsed by distilled water and acetone. The graphite and Saturated Calomel Electrode (SCE) were chosen as axillary and reference electrode respectively. Before each test, the electrodes were immersed in the solution for 15 minutes for reaching the stable potential. The Tafel polarization was performed from -200 mV to +200 mV in respect of open circuit potential (OCP) with a potential scan rate of 1 mV/s. Corrview software was used for the calculation of anodic and cathodic Tafel slopes, corrosion current density and corrosion potential.

The current efficiency of sodium ferrate production (η) is given by equation 7. The value of C_{the} is calculated by equation 8 according to faradic law.

$$\eta(\%) = \frac{C_{exp}}{C_{the}} \times 100 \quad (7)$$

Where

C_{exp} is the concentration of produced sodium ferrate in the experiments and

C_{the} is the concentration of produced sodium ferrate calculated by faradic law

$$C_{Theor} = MIt/nF \quad (8)$$

Where I is the applied current intensity (A), t is the test duration (s), F is the faradic constant (96485 $c.mol^{-1}$), M is the molar mass of sodium ferrate ($g.mol^{-1}$), and n is the number of electrons present in reaction [1, 9].

One of the effective parameters in sodium production cost is the consumed power during the production process which is calculated by equation 9:

$$E.C = VIt/m \quad (9)$$

Where V is the potential difference (V), t is the test duration (h), I is the applied current intensity (A), m is the produced sodium ferrate (kg) and E.C is the consumed energy (kWh/kg) [1, 9].

To investigate the effects of different parameters on current efficiency and concentration of sodium ferrate production, the UV-Visible spectroscopy is mostly used. The absorption spectrum of the aqueous solution of sodium ferrate has a distinct color of violet and is close to infra-red, with a wavelength of 450 to 600 nm.

This spectrum has the maximum absorption at wavelength of 505 nm for sodium ferrate solution [1, 9, 23-29].

In preliminary measurements, it is found that the maximum absorption of sodium ferrate happens at the wavelength of 505 nm; so, based on this result, the entire concentration calculation was done at the wavelength of 505 nm. Then after the measurement of maximum absorption, for converting the absorption value to the concentration, the calibration curve was employed (Figure 1).

Equation (10) was used to obtain the purity of sodium ferrate particles. Thus, mix the appropriate amount of produced sodium ferrate powder in each step in 100 mL saturated aqueous NaOH for 5 minutes at 400 rpm and 10 ℃ and then some of the electrolyte from the upper part of the container was analyzed by an ultraviolet-visible spectrometer. [29].

$$K_2FeO_4\ Purity = \frac{A}{\varepsilon} \times 0.1 \times \frac{M}{Wight\ of\ Sample} \times 100\% \quad (10)$$

In Equation (10) ε, is the Attenuation coefficient which is determined from Figure 1 (calibration curve, absorbance vs. concentration) using the Beer-Lambert law (equation 11), M is the molecular mass of sodium ferrate. In fact, the A/ε shows the concentration of sodium ferrate particles in the electrolyte (assuming a cell width of 1 cm).

$$A = \varepsilon LC \quad (11)$$

A is absorbance (without unit), L is cell length (cm), ε is the attenuation coefficient of sodium ferrate ($M^{-1}cm^{-1}$) and C is Concentration (M) [30].

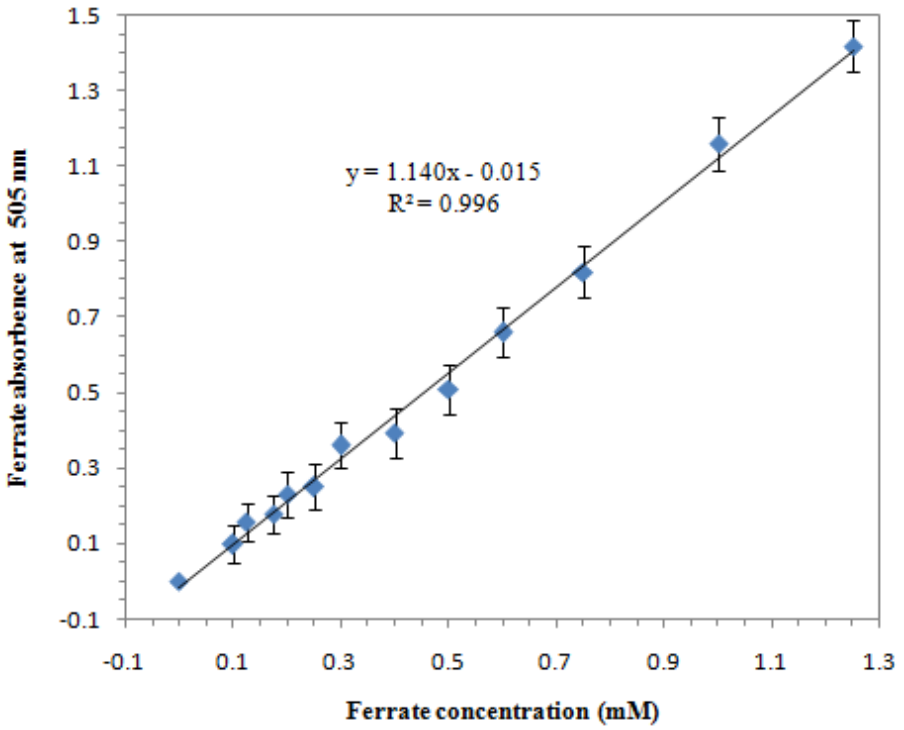

Fig. 1. Calibration Curve of sodium ferrate measurement in 16 M NaOH.

For analysis and morphological observation, X-ray diffractometry (XRD) (Philips PW3040) and Scanning Electron Microscope (SEM) (TESCAN MIRA3) were employed. The synthesized powders extracted from the suspension by the following method. The NaOH solution removed using Buchner Funnel and Vacuum Suction and the powders washed four times by n-pentane, n-hexane, isopropyl alcohol, and diethyl ether. Subsequently, the particles are kept in a vacuum of less than 30 mmHg for 2 hours to dry completely [29].

3. Results and Discussion

3.1. UV- visible spectroscopy of sodium ferrate

The UV-Visible spectroscopy results as it is shown in Figure 2, revealed that the maximum absorption is about 505 nm (peak of absorption). The presence of the absorption peak indicates the existence of sodium ferrate in the solution [1, 9, 24-28, 30]. Despite that, in some tests, the absorption peak shifts to upper or lower wavelength which can indicate changes in particle size [31, 32].

Figure 2- The maximum absorption based on the wavelength of UV-Visible spectroscopy.

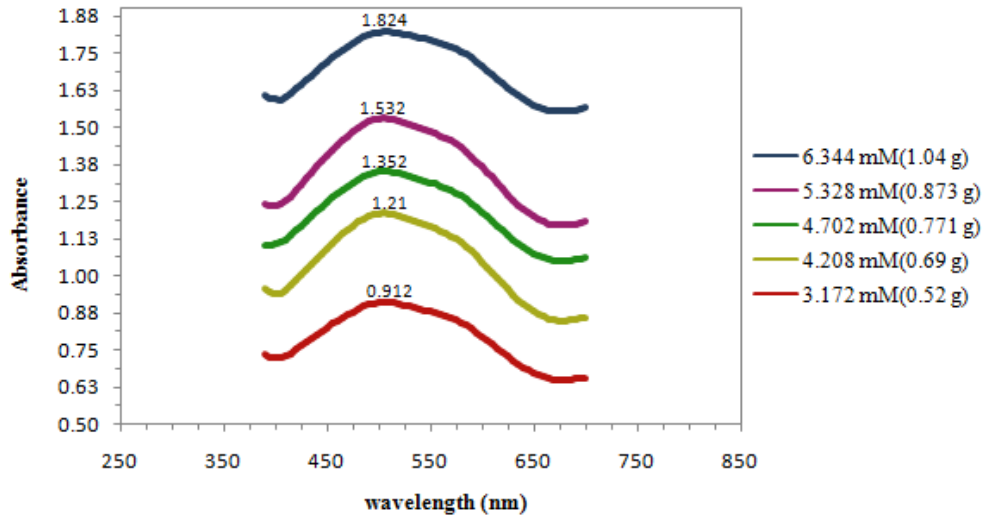

Fig. 2. The maximum absorption based on the wavelength of UV-Visible spectroscopy.

Table 2. The relation between current density and current efficiency and energy consumption in sodium ferrate production by electrochemical method.

row	Current (A)	Potential (V)	Current density ($mA.cm^{-2}$)	Sodium ferrate concentration (mM)	Sodium ferrate concentration C_{exp} (g)	Sodium ferrate concentration C_{the} (g)	Current efficiency (%)	Energy consumption (kwh/kg)
1	1.5	2.84	65.78	1.19	0.195	0.765	25.46	10.93
2	0.75	2.42	32.89	0.92	0.150	0.382	39.25	6.04
3	0.25	2.02	10.96	0.52	0.085	0.127	66.95	2.96
4	0.18	1.95	7.89	0.41	0.068	0.092	74.15	2.58
5	0.09	1.92	3.94	0.22	0.036	0.046	78.16	2.41
6	0.045	1.9	1.97	0.11	0.018	0.023	76.85	2.43

3.2. Determination of optimum condition of sodium ferrate synthesis

The current density

The current efficiency of sodium ferrate production in 14 M NaOH at temperature of 35 ^{o}C at various current densities and duration of 30 m has been tested and the results are shown in Table 2. According to Table 2, the highest current efficiency and the lowest energy consumption were achieved with a current density of 3.94 $mAcm^{-2}$.

In current densities less than 3.94 $mAcm^{-2}$, due to low anodic potential, the sodium ferrate production process happens at a lower rate. Furthermore, with more current density, the amount of sodium ferrate has been reduced. By increasing the current density three effects happen:

1- Ling [14] considers that, by increasing the current density to the values more than the optimum level, the temperature of the electrolyte increases due to more heat dissipation and makes more

sodium ferrate decomposition and therefore, the production rate will decrease in higher current densities. But in this research, due to the control of electrolyte temperature to maintain below 35 °C by using water cooling system, this not happens.

2- Barisci and coworkers [1] supposed that by increasing the current density, a large portion of current spends for reactions other than anodic dissolution. Actually, the oxygen [1, 33] and hydrogen [1, 9] reduction reactions consume a large part of the current and this decreases the sodium ferrate production rate.
3- In low current densities, the passivation process delayed. By increasing the current density, the passive layer forms in less time duration [7, 34].

As can be seen in Figure 3, in current densities more than optimum, the slope of the curve falls considerably and the curve shows a logarithmic behavior. It can be attributed to the decline in sodium ferrate production rate due to growth in anode passivation rate with time and or increase in reduction reactions of hydrogen and oxygen in current densities of greater than optimum.

Electrolyte concentration

After the determination of optimum current density, sodium ferrate synthesis has been studied with a current density of 3.94 $mA.cm^{-2}$, temperature of 35 °C and various electrolyte concentrations. According to the UV-visible spectroscopy results (Table 3), the highest amount of sodium ferrate in the electrolyte was achieved in 16 M NaOH. By increasing in concentration of NaOH from 8 to 18 M, the electrical conductivity declines and OH^- ion concentration increases and free water in electrolytes decreases [6]. An increase in OH^- ion concentration leads to enhance the production rate according to equation 1, the reduction of electrical conductivity and free water leads to a decline in synthesis rate. It seems that the optimum condition occurs in 16 M NaOH electrolyte.

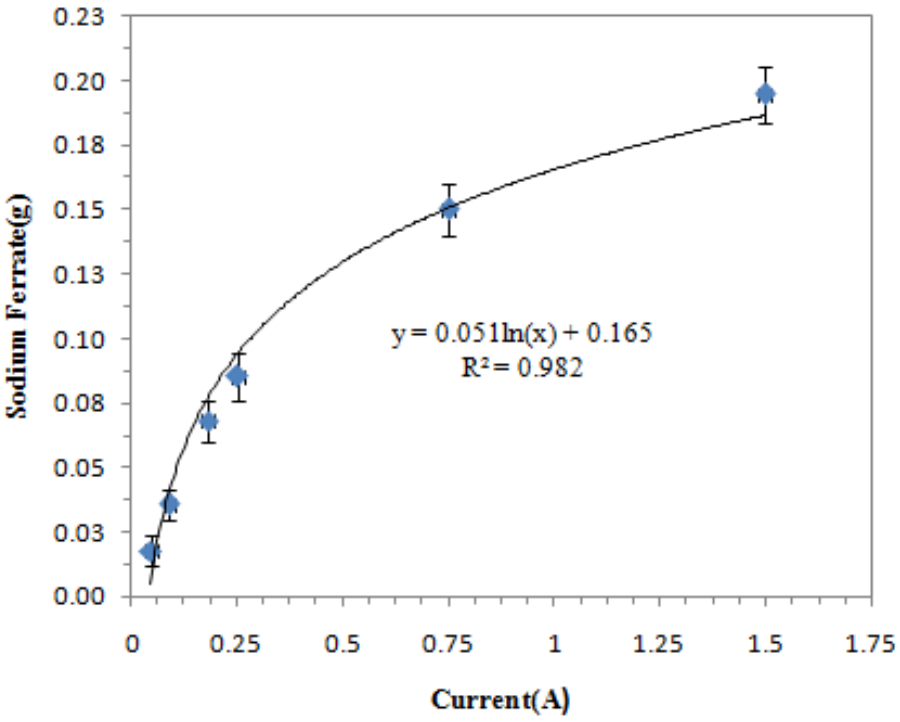

Fig. 3. The amount of produced sodium ferrate at an initial temperature of 35 °C, 14 M NaOH electrolyte and various applied current densities.

Table 3. The relation between the concentration of NaOH in the electrolyte with current efficiency and energy consumption in sodium ferrate synthesis by electrochemical method.

row	NaOH Concentration (M)	Potential (V)	Sodium ferrate concentration (mM)	C_{exp} (mg)	Current efficiency (%)	Energy consumption (kwh/kg)
1	8	1.14	0.08	13	27.51	4.07
2	10	1.43	0.13	21	45.41	3.09
3	12	1.67	0.18	29	62.19	2.55
4	14	1.92	0.22	36	78.16	2.41
5	16	1.96	0.23	39	84.28	2.28
6	18	2.01	0.21	34	73.80	2.67
7	21	2.08	0.13	22	47.16	4.33

The potentiodynamic polarization tests were performed at various NaOH concentration and temperature of 35 ºC (Figure 4). The results showed that the highest corrosion rate belonged to the 16 M NaOH and afterward 14 and 18 M respectively (Table 4). This result justifies the values in table 3.

In 8 M NaOH electrolyte, according to equation 6, due to the high volume of water, the synthesized sodium ferrate particles are extremely unstable and decompose rapidly. Accordingly, the energy consumption significantly intensifies because a considerable amount of sodium ferrate decomposes immediately after synthesis. On the other hand, in 18 and 21 M electrolytes, due to a decrease in free water activity, the corrosion rate and sodium ferrate decomposition are minor [33]. Based on these two reasons, iron II and III valence are stable besides sodium ferrate particles in the electrolyte [6, 35].

Electrolyte temperature

After finding the optimum current density and electrolyte concentration, the synthesis of sodium ferrate has been investigated with a current density of 3.94 mA.cm^{-2} and 16 M NaOH at different temperatures. The results of UV-Visible spectroscopy (Table 5) showed that the highest amount of sodium ferrate synthesis was achieved at 50 ºC. The OH^- activity and electrolyte conductivity accelerate by increasing in temperature which enhances the rate of sodium ferrate production. On the other hand, an increase in temperature leads to more sodium ferrate decomposition but it seems that the optimum condition happens at 50 ºC temperature. In upper temperatures, the rate of decomposition goes beyond the rate of synthesis.

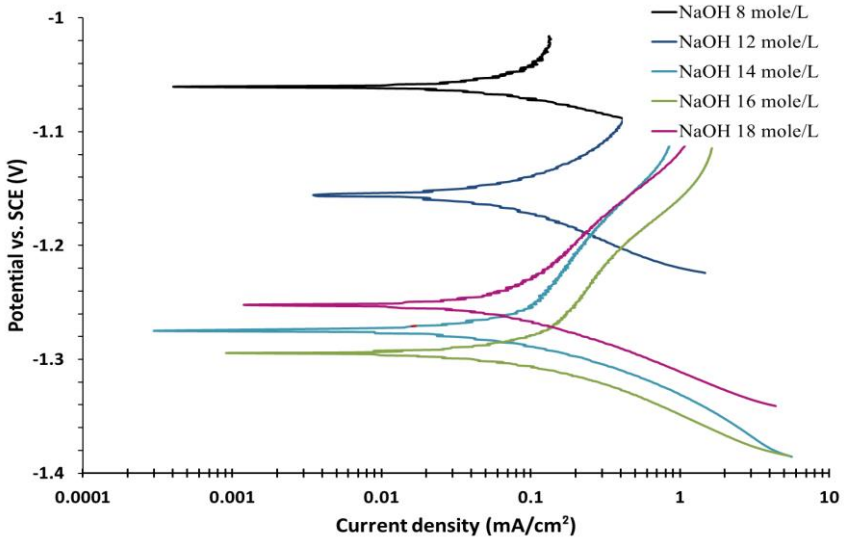

Fig. 4. Tafel polarization curves of low carbon steel in NaOH electrolyte with various concentration at 35 ºC.

Table 4. Corrosion parameters extracted from Figure 3.

row	NaOH Concentration (M)	β_a (mV/decades)	β_c (mV/decades)	Corrosion Current Density ($\mu A.cm^{-2}$)	Corrosion Potential vs. SCE (mV)	Corrosion Rate (mpy)
1	8	56	-25	8.9	-863	8.19
2	12	57	-49	12.2	-959	11.21
3	14	140	-46	16.1	-1079	14.77
4	16	131	-49	21.2	-1099	19.39
5	18	111	-49	15.8	-1055	14.49

Table 5. The relation between initial temperature and current efficiency and energy consumption in sodium ferrate synthesis by electrochemical method.

row	Electrolyte Temperature (°C)	Potential (V)	Sodium ferrate concentration (mM)	C_{exp} (mg)	Current efficiency (%)	Energy consumption (kwh/kg)
1	10	2.48	0.05	7	15.28	15.92
2	20	2.19	0.11	18	39.30	5.47
3	30	2.01	0.18	29	63.32	3.11
4	35	1.96	0.23	39	84.28	2.28
5	40	1.88	0.25	41	89.52	1.85
6	50	1.79	0.26	42	91.70	1.91
7	60	1.72	0.24	39	85.15	1.98
8	75	1.65	0.13	21	45.85	3.53

The polarization tests in 16 M NaOH have performed at various temperatures. The given results in table 6 show that the corrosion rate in 50 °C is more than that in 35°C. It is because of escalating in OH^- ion activity which prevents the passive layer formation or dissolves any formed passive film. So, at the temperature of 50 °C, the effect of anode passivation on current efficiency was small and can be neglected. In this situation, the sodium ferrate decomposition and increased in the ratio of cathodic reaction rates to the anodic dissolution rates reduce current efficiency and augments energy consumption.

Table 6. Corrosion parameters of low carbon steel in 16 M NaOH electrolyte at various temperatures.

row	Solution Temperature (°C)	β_a (mV/decades)	β_c (mV/decades)	Corrosion Current Density ($\mu A.cm^{-2}$)	Corrosion Potential vs. SCE (mV)	Corrosion Rate (mpy)
1	50	112	-52	34.6	-1093	31.73
2	35	132	-49	21.2	-1055	19.39
3	27	106	-53	10.4	-1029	9.56

The weight loss test has performed on anode for 30 minutes at different temperatures. It was expected for the sodium ferrate production rate to increase with initial temperature due to higher electrical conductivity and OH^- activity. Results in Figure 5 demonstrated that, by increasing temperature from 10 to 50 °C, the weight loss during the test has also elevated which is attributed to more anode dissolution with higher electrolyte temperature. From 50 to 75 °C, the extent of weight loss (anode dissolution) has reduced. This showed that the increment of in

electrolyte temperature to values more than 50 °C, the further current between anode and cathode spent for reactions rather than anode dissolution. In other words, the cathodic reaction has intensified also, by increasing temperature up to 50 °C, a large portion of the current is taken by cathodic reactions and less current for anodic reactions. Based on the produced sodium ferrate, the theoretical weight loss has been calculated. By comparing the theoretical weight loss with measured weight loss of anode, it was seen that higher electrolyte temperature up to 35 °C the measured weight loss and the theoretical weight loss has about 0.3 mg difference which can be attributed to the error in measurement in weight loss method or UV-Visible spectroscopy. For electrolyte temperatures of 40, 50, 60 and 70 °C the differences between results from the measured weight loss and the theoretical weight loss were achieved 0.4, 0.6, 1.0 and 4.4 mg. The measured weight loss is more than the calculated one. It means that at temperatures above 50 °C, more sodium ferrate should be detected due to more decomposition of Sodium ferrate by an increase in temperature during 30 minutes were lost. The higher energy consumption at 50 °C in comparison with 40 °C is also because of more decomposition of Sodium ferrate at the temperature of 50 °C as compared with 40 °C for 30 min of synthesis.

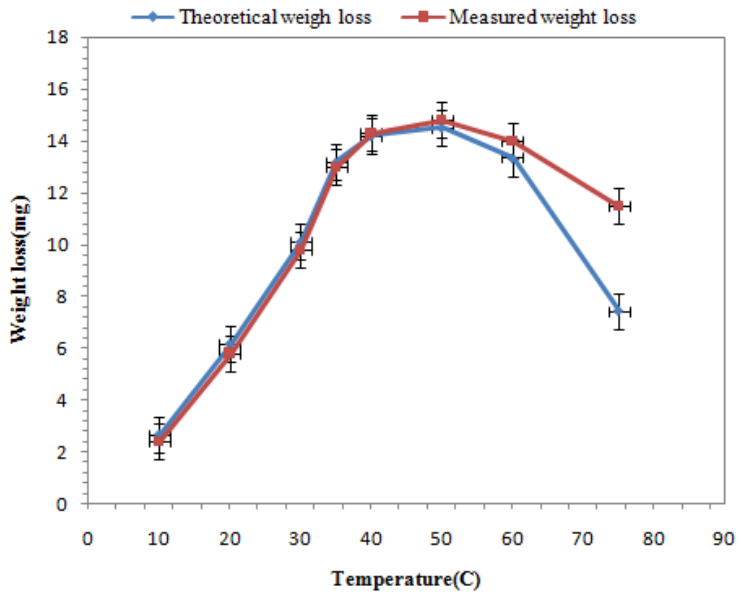

Fig. 5. The changes in weight loss of anode in sodium ferrate generation with 7.89 $mA.cm^{-2}$ current density, 16 M NaOH electrolyte for 30 m at various temperatures.

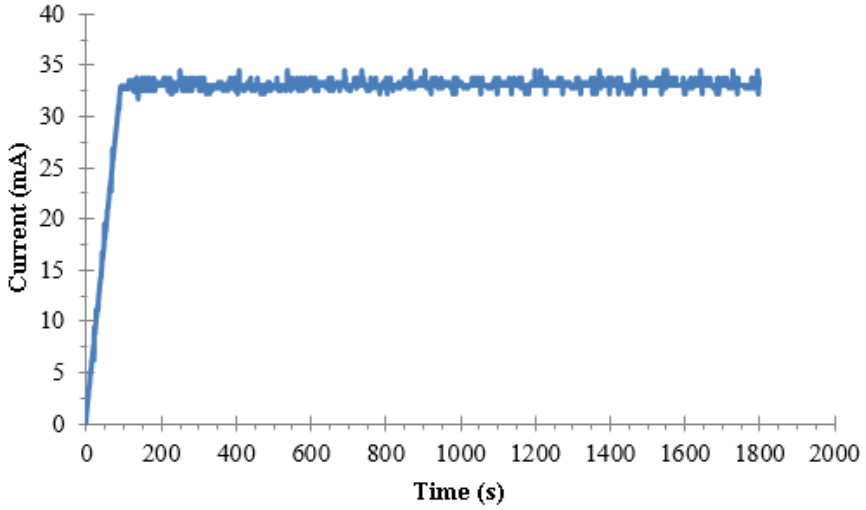

Fig. 6. The current – time curve for the synthesis of sodium ferrate at 1.79 V, 16 M NaOH, and 50 °C

Optimization

Figure 6 shows the current changes over time under optimal production conditions (16 M NaOH, 50 ºC and 1.79 V). In the beginning, the current increases sharply and the gas evolution occurs at the electrode surface and the electrolyte gradually becomes purple. At this time the current reaches a constant value and its oscillations decrease. The level of this constant current depends on the electrolyte resistance and the polarization of the electrode surface.

The XRD patterns and SEM images of the sodium ferrate synthesized under optimum conditions and for 0.5 h are presented in Figures 7 and 8, respectively. All peaks in the pattern associated with synthesized sodium ferrate. In the continuous synthesis of ferrate (VI), a series of by-products including iron hydroxide ($Fe(OH)_3$) and oxide compounds forms during the electrolysis. Moreover, by increasing the viscosity of the fluid due to more production, carbon dioxide gas is absorbed into the liquid and forms the sodium bicarbonate phase (Na_2CO_3) [29]. As it is explained above due to the good sealing and short production time, the Na_2CO_3 and other iron oxides and hydroxide are not present in the synthesized and dried powder.

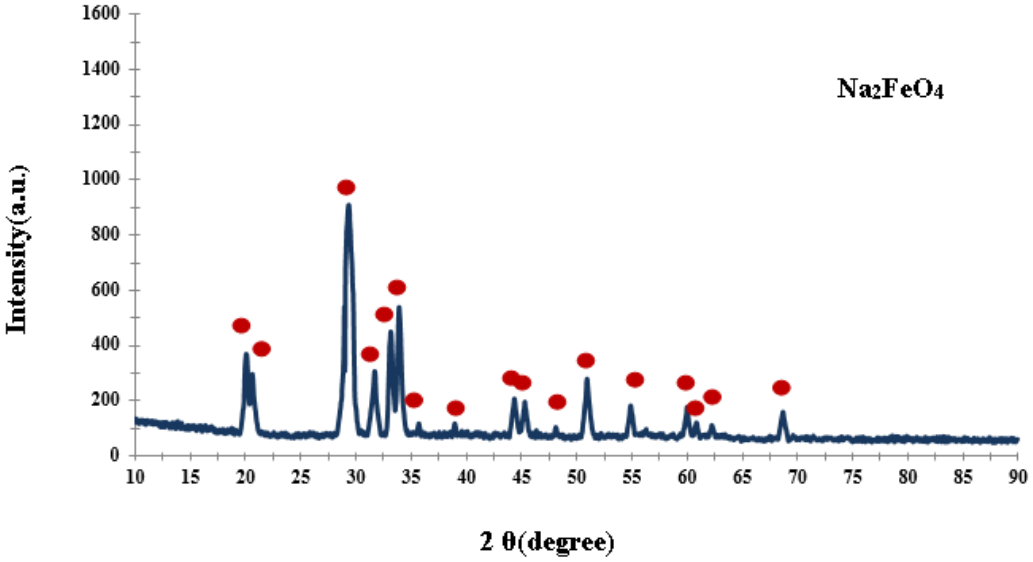

Fig. 7. X-ray diffraction patterns of sodium ferrate synthesized at optimum condition.

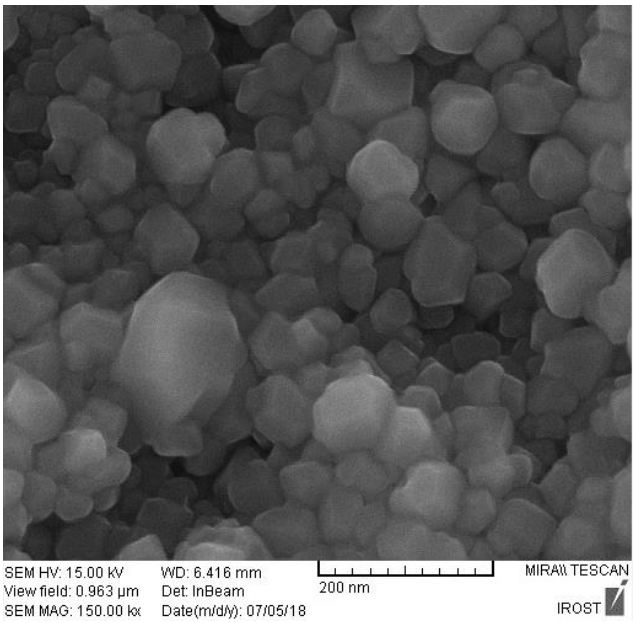

Fig. 8. SEM image of sodium ferrate synthesized at optimum condition.

Also, the absence of impurities in the synthesized powder can confirm the optimum production conditions. The SEM image of the sodium ferrate particles synthesized throughout 0.5 h shows a uniform morphology and polyhedral structure with a size of less than 100 nm.

The purity of sodium ferrate in solution was measured 99.5% using equation 10. Also, energy dispersive spectroscopy (EDS) analysis was performed on SEM images at different points of the synthesized particles and the results showed that the average particle purity was more than 99%. The impurity may be attributed to the presence of a few amounts of sodium hydroxide with the sodium ferrate nanoparticles.

4. Conclusions

Energy consumption and current efficiency of sodium ferrate generation by the electrochemical method with different production condition has been investigated. In the present study, the applied current density, NaOH concentration in electrolyte and temperature was examined at fixed 30 minutes of synthesis time. The optimum situation was achieved with a current density of 3.94 $mA.cm^{-2}$, 16 M NaOH concentration, and a temperature of 50 ^{o}C. In an optimized condition, the current efficiency and energy consumption reached 91.7% and 1.91 kwh/kg, respectively. With temperature and applied current density above optimum, the current efficiency reduced and energy consumption accelerate due to an increase in cathodic reaction rates in comparison with anodic dissolution reactions and an increase in the decomposition of ferrate (VI) compounds. At a concentration above 16 M of NaOH, due to more viscosity of electrolyte, the electrical conductivity and therefore free water decreases which lessens production rate. As well, energy consumption is related to solution electrical resistivity and mass of produced sodium ferrate. However, sodium ferrate production happens at less potential and consumes, more production has been generated.

References

[1] S.Barışçı, F. Ulu, H. Sarkka, A. Dimoglo, M. Sillanpaa, “Electrosynthesis of Ferrate (VI) ion using high purity iron electrodes: optimization of influencing parameters on the process and investigating its stability”, Int J Electrochem Sci., Vol. 9, 2014, pp. 3099-3117.

[2] W. He, J. Wang, C. Yang, J. Zhang, “The rapid electrochemical preparation of dissolved ferrate(VI): Effects of various operating parameters”, Electrochimica Acta, vol. 48, 2006, pp. 1967-1973.

[3] M. De Koninc, D. Belanger, “The electrochemical generation of ferrate at pressed iron powder electrode: comparison with a foil electrode”, Electrochimica acta, Vol. 48, 2003, pp. 1435-1442.

[4] J.R. López, D.C.P Fong, P.F.M Herrera, S.P. Sicairos, I.C. Ayala, J.R.O. del Castillo, “Potassium Ferrate and/or Sodium Ferrate Generation Using a Prototype of Electrochemical Reactor without Membrane”, ECS Transactions, Vol. 15, 2008, pp. 403-410.

[5] K. Bouzek, M.J. Schmidt, A.A. Wragg, “Influence of electrolyte composition on current yield during ferrate (VI) production by anodic iron dissolution”, Electrochemistry communications, Vol. 1 1999, pp. 370-374.

[6] M. De Koninck, T. Brousse, D. Bélanger, “The electrochemical generation of ferrate at pressed iron powder electrodes: effect of various operating parameters”, Electrochimica Acta, Vol. 48, 2003, pp. 1425-1433.

[7] W. He, H. Shao, Q. Chen, J. Wang, J. Zhang, “Polarization Characteristic of Iron Anode in Concentrated NaOH Solution”. Acta Physico-Chimica Sinica, Vol. 23, 2007, pp. 1525-1530

[8] Z. Macova, K. Bouzek, J. Híveš, V.K. Sharma, R.J. Terryn, J.C. Baum, “Research progress in the electrochemical synthesis of ferrate (VI)”, Electrochimica acta, Vol. 54, pp. 2673-2683.

[9] M, Alsheyab, J-Q Jiang, C. Stanford, “Electrochemical generation of ferrate (VI): Determination of optimum conditions”, Desalination, Vol. 254, 2010 pp. 175-178.

[10] A. Talaiekhozani, M. Bagheri, M.R. Talaei, N. Jaafarzadeh, “An Overview on Production and Applications of Ferrate (VI)”. Jundishapur Journal of Health Sciences, 2016.

[11] D. Tiwari, S.M. Lee, “Ferrate (VI) in the treatment of wastewaters: a new generation green chemical”, INTECH Open Access Publisher, 2011.

[12] Nguema PF, Jun M. “Application of Ferrate (VI) as Disinfectant in Drinking Water

Treatment Processes: A Review". Intl J. 2016;7:53-62.
[13] J-Q. Jiang, H.B. Durai, M. Petri, T. Grummt, R. Winzenbacher, "Drinking water treatment by ferrate (VI) and toxicity assessment of the treated water", Desalination and Water Treatment, 2016, pp. 1-7.
[14] L. Ding, Removal of methyl mercaptan from foul gas by in-situ production of ferrate (VI) for odour control, Ph.D. Thesis, University of Hong Kong Polytechnic, Hong Kong, 2013
[15] V. Shastry, "Waste Water Treatment Using Eco Friendly Oxidising Agent Fe (VI)", Hydrology: Current Research, Vol. 2, 2011, pp. 1- 4.
[16] M. Kooti, M. Jorfi, H. Javadi, "Rapid chemical synthesis of four ferrate (VI) compounds", Journal of the Iranian Chemical Society, Vol. 7, 2010, pp. 814-819.
[17] K. Manoli, G. Nakhla, A.K. Ray, V.K. Sharma, "Enhanced oxidative transformation of organic contaminants by activation of ferrate(VI): Possible involvement of FeV/FeIV species", Chemical Engineering Journal, Vol. 307, 2017, pp. 513-517.
[18] B.F. Monzyk, J.A. Ford, J.T. Stropki, D.N. Clark, V.V. Gadkari, K.P. Mitchell. "Corrosion resistant primer coating", Google Patents, 2014.
[19] T. Burleigh, P. Schmuki, S. Virtanen, "Properties of the Nanoporous Anodic Oxide Electrochemically Grown on Steel in Hot 50% NaOH", Journal of The Electrochemical Society, Vol.156, 2009, pp.45-53.
[20] M. Sánchez-Moreno, H. Takenouti, J.J. García-Jareño, F. Vicente, C. Alonso, "A theoretical approach of impedance spectroscopy during the passivation of steel in alkaline media". Electrochimica Acta, Vol.54, 2009, pp. 7222-7226.
[21] A. Fattah-alhosseini , M.M. Khalvan, "Semiconducting properties of passive films formed on AISI 420 stainless steel in nitric acid solutions", Journal of Advanced Materials and Processing, Vol. 1, 2013, pp. 15-22.
[22] A. Fattah-alhosseini, M.A. Sonamia, A. Loghmani, F.Z. Shoja, "Passivity of AISI 316L stainless steel as a function of nitric concentration", Journal of Advanced Materials and Processing, Vol. 2, 2014, 21-30.
[23] J-Q. Jiang, C. Stanford, M, Alsheyab, "The online generation and application of ferrate (VI) for sewage treatment—A pilot scale trial", Separation and Purification Technology, Vol. 68, 2009, pp. 227-231.
[24] C. Stanford, J-Q. Jiang, M. Alsheyab, "Electrochemical production of ferrate (iron VI): application to the wastewater treatment on a laboratory scale and comparison with iron (III) coagulant", Water, Air, & Soil Pollution, Vol. 209, 2010, pp. 483-488.
[25] Z. Minevski, J. Maxey, C. Nelson, D. Taylor, "Electrochemical method and apparatus for producing and separating ferrate (VI) compounds", Google Patents; 2005.
[26] J-Q. Jiang, B. Lloyd, "Progress in the development and use of ferrate (VI) salt as an oxidant and coagulant for water and wastewater treatment", Water research, Vol.36, 2002, 1397-1408.
[27] M. Alsheyab, J-Q. Jiang, C. Stanford. "Risk assessment of hydrogen gas production in the laboratory scale electrochemical generation of ferrate(VI)", Journal of Chemical Health and Safety, Vol. 15, 2008, pp. 16-20.
[28] S.N. Licht, V. Halperin, L. Naschitz, N. Halperin, L. Lin, J. Chen, L. Nadezhda, C. Lin, S.J. Ghosh, B. Liu, "Analysis of ferrate (VI) compounds and super-iron Fe (VI) battery cathodes: FTIR, ICP, titrimetric, XRD, UV/VIS, and electrochemical characterization", Journal of Power Sources, Vol. 101, 2001, pp.167-176.
[29] A.D.P. Rios, Dewatering of Biosolids by Sodium Ferrate, Ph.D. Thesis, University of Central Florida Orlando, Florida, 2004.
[30] D. Ghernaout, M. Naceur, "Ferrate (VI): In situ generation and water treatment–A review", Desalination and Water Treatment, Vol. 30, 2011, pp. 319-332.
[31] A. Watthanaphanit, Y.K. Heo, N. Saito, "Influence of the discharge time of solution plasma process on the formation of gold nanoparticles in alginate matrix", Journal of the Taiwan Institute of Chemical Engineers, Vol. 45, 2014, pp. 3099-3103.
[32] W, Haiss, N.T.K. Thanh, J. Aveyard, D.G. Fernig, "Determination of Size and Concentration of Gold Nanoparticles from UV−Vis Spectra", Analytical Chemistry, Vol. 79, 2007, pp. 4215-4221.
[33] X. Yu, S. Licht, "Advances in electrochemical Fe (VI) synthesis and analysis", Journal of Applied Electrochemistry, Vol.38, 2008, pp. 731-742.

[34] Z. Ding, C. Yang, Q. Wu, "The electrochemical generation of ferrate at porous magnetite electrode", Electrochimica Acta, Vol. 49, 2004, pp. 3155-3159.
[35] K. Bouzek, I. RouŠAr, " Influence of anode material on current yield during ferrate(vi) production by anodic iron dissolution: Part III: Current efficiency during anodic dissolution of pure iron to ferrate(vi) in concentrated alkali hydroxide solutions", Journal of Applied Electrochemistry, Vol. 27, 1997, pp. 679-684.